IMMIGRANT AND NATIVE ROCKS IN SIMPLE CRATERS: A NEW METHOD FOR DATING AIRLESS SURFACES

L. Rubanenko[1], T. M. Powell[1] and D. A. Paige[1] University of California, Los Angeles, CA, USA (liorr@ucla.edu)

Introduction: Dating airless surfaces is most commonly achieved by measuring the impact crater density [e.g 1, 2, 3]. However, these methods require sampling a large number of craters and are prone to human errors and lighting biases. Rocks, along with the craters that harbor them, are constantly being degraded by meteorites impacting the surface, removing material and reworking it to produce fine regolith. This degradation is often described as a diffusive process [4, 5], in which larger features erode on longer timescales than smaller features. The Diviner Radiometer experiment on board the Lunar Reconnaissance Orbiter (LRO) measures the rock abundance (RA) by sensing the higher thermal conductivity of rocks compared to regolith [6]. These data were later used for crater dating by correlating the 95^{th} percentile of the RA distribution (RA_{95}) to known crater radiometric ages [7]. However, this technique is not sufficiently sensitive to determine the age of craters older than $\sim$ 1 Ga, whose RA_{95} is of the order of a percent and is heavily influenced by the material properties and regolith thickness. Additionally, "immigrant" rocks brought into the surface as a result of other impacts may cause an old, degraded crater to appear fresh. Here we present a novel surface dating method by establishing a link between the rock abundance probability density function (PDF) and the relative age of the surface. We incorporate Diviner derived rock abundance maps with a recently published extensive crater catalog [8] in order to date the lunar surface. Our method can distinguish between craters older than $\sim$ 1 Ga and is less sensitive to the material properties, as the slope of the PDF depends on the initial power-law rock production function. Finally, we compare the 95_{th} percentile rock abundance data and the slope of the PDF in log-log space, and distinguish between "native" rocks formed during the crater formation and "immigrant" rocks, rocks brought to the crater by neighbouring impacts.

Methods: In order to measure the RA for lunar craters we use the global RA map gridded at 128 px/deg published on the Planetary Data System. We only use measurements conducted between $70°\mathrm{S} - 70°\mathrm{N}$, as in high latitudes permanently shadowed regions skew the results by affecting the measured thermal conductivity [6]. In addition, we measure craters' depth/diameter (d/D) across three topographic profiles extracted from the Lunar Orbiter Laser Altimeter (LOLA) map gridded at 120 m/px (also see [9]). We restrict our d/D measurements to $60°\mathrm{N/S} - 70°\mathrm{N/S}$ due to the higher LOLA resolution in these latitudes, but plan to expand this range in the future.

Calculating the crater RA probability density function: For each crater in the catalog [8] we extract the rock abundance map and calculate the probability density function (PDF); the normalized frequency of RA pixels. We chose to focus on simple craters with diameters $\sim 3 - 15$ km, but plan to extend this range to smaller craters. Upon crater formation, the PDF will follow a power law production function. With time, erosion would act to move the PDF towards lower RA values and change its slope - as pixels with high RA turn into pixels with low RA. Figure 1 shows the rock abundance PDF for three craters in three degradation states. As craters degrade, rock abundance decreases and the slope of the PDF in log-log space becomes steeper (blue line compared to green line). In the intermediate stage we find the PDF becomes bilinear. This is potentially caused by a temporary increase in the rock abundance that occurs when broken rock fragments cover a larger fraction of the pixel than the original cohesive rock from which they were separated. Alternatively, the RA_{95} of pixels containing mostly small rocks may decrease more rapidly as rock fragment size approaches the diurnal skin depth and the detection limit of Diviner.

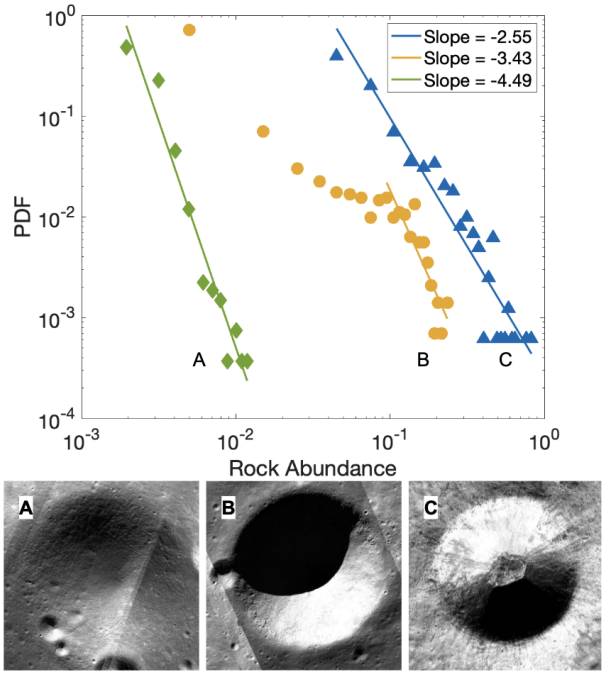

Figure 1: The probability density function of three craters in three different degradation states: heavily eroded (A), intermidiate (B) and fresh (C).

Link between crater d/D and RA: Impacts erode rocks inside and around craters and reduce their d/D ratio by mass wasting and infill from nearby impact ejecta. In order to compare the rates of these two parallel processes we correlate the d/D ratio with the 95_{th} percentile rock abundance (Figure 2). We find, as expected, that smaller craters ($\sim 3 - 4$ km) degrade and lose their rocks at a comparable rate (move diagonally left-down in Figure 2 while larger craters first lose their rocks (move down in Figure 2) and then become shallower (move left in Figure 2). Additionally, we find that below a few percent RA_{95} it is difficult to distinguish between fresh (high d/D) and eroded (low d/D) craters. To overcome this, we develop a new dating technique using the entire probability density function.

Dating surface using rock abundance: as shown above, dating craters using their RA_{95} value is inaccurate for craters older than $\sim$ 1 Ga and is heavily influenced by the material properties and regolith thickness. Additionally, rocks reach-

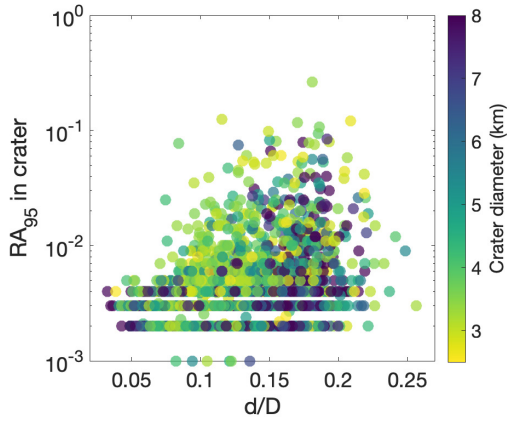

Figure 2: Erosion causes craters to lose their rocks (move down on the diagram) and makes them shallower (move left on the diagram). Craters with diameters $\sim 3-4$ km become shallow and lose their rocks at a comparable rate (move diagonally), while larger craters first lose their rocks and then become shallow.

ing the measured crater from adjacent impacts can increase its RA_{95}, disguising old craters as fresh craters. Here we use the slope of the RA PDF in log-log scale to improve crater dating through rock abundance. By comparing this slope to RA_{95}, we are able to distinguish between rocks that form in situ following the impact ("native" rocks) and rocks that reached the crater long after it formed ("immigrant" rocks). At a steady state, we can assume constant flux: immigrant rocks ejected from nearby impacts will contribute an equal amount of rock per unit area to the crater. Even though the same rock mass is added to each pixel within the crater, the relative effect of this addition on pixels with low rock abundance will be greater than on pixels with high rock abundance, making the slope of the rock abundance PDF steeper. Consequently, craters whose RA PDFs have a steep slope in log-log scale *and* a high RA_{95} value mostly likely harbor immigrant rocks. Craters whose RA PDFs have a shallower slope but low RA_{95} value are most likely old and contain native rocks. Fresh craters will present both a shallow PDF slope and high RA_{95}. Figure 3 shows three maps of the lunar surface: RA_{95} (top), the slope of the RA PDF (middle) and crater density (bottom) for simple craters $3-15$ km. To produce these maps, we binned craters in spatial bins of $2^\circ \times 2^\circ$ and calculated the mean RA_{95} and mean RA PDF slope at each bin. The ratio of rocky to non-rocky craters on older surfaces is lower compared to younger surfaces. Consequently, younger surfaces will have, on average, a higher RA_95 and a shallower PDF slope than older surfaces. For example, the RA_{95} of craters along the path of Giordano Bruno's (GB) ejecta are higher than other craters in the region despite similar expected regional and crater ages. This is likely due to the addition of ejected rocky material into older craters. Our RA PDF power map does not show GB related features; the addition of some rock abundance to all pixels steepens the RA PDF slope (young rocky crates have shallow slopes). This allows us to differentiate between high rock abundance due to native and immigrant rocks.

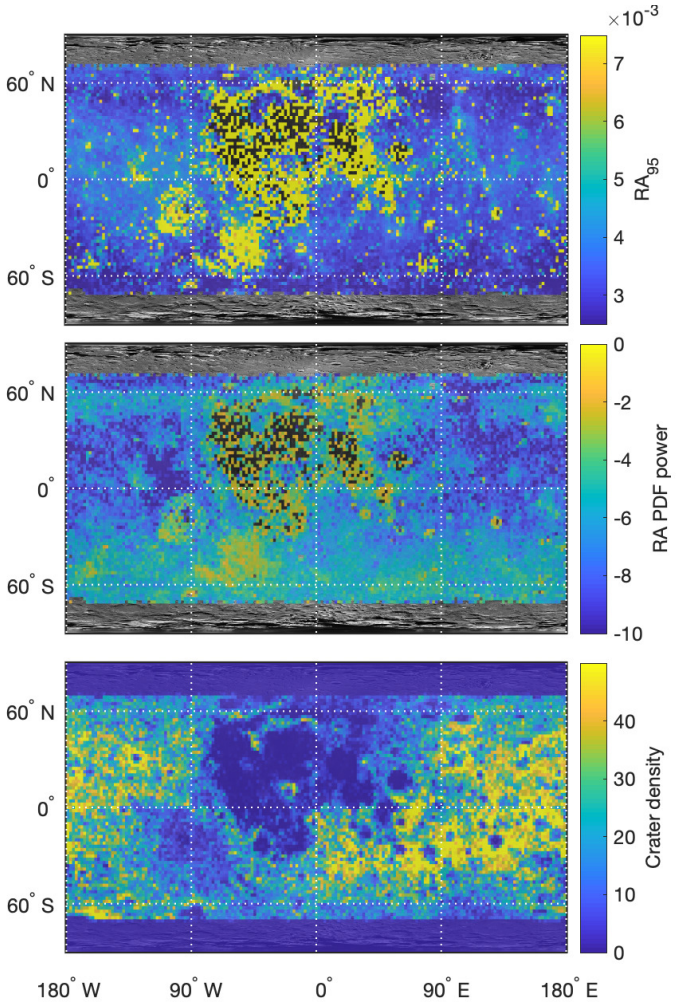

Figure 3: Top: RA_{95}, middle: rock abundance PDF power (slope in log-log space) and bottom: crater density map for simple lunar craters 3-15 km. The age of the surface is better predicted by the power of the rock abundance PDF than only its 95_{th} percentile. In order to prepare this figure we binned craters at $2^\circ \times 2^\circ$ spatial bins and calculated the average RA_95 and slope in each bin.

References

[1] Gerhard Neukum et al. In *Chronology and evolution of Mars*. 2001.
[2] Crater Analysis Techniques Working Group et al. *Icarus*, 37:467–474, 1979.
[3] J-P Williams et al. *Meteoritics & Planetary Science*, 53: 554–582, 2018.
[4] Howard P Ross. *JGR*, 1968.
[5] C.I. Fassett and B.J. Thomson. *JGR: Planets*, 2014.
[6] J.L. Bandfield et al. *JGR: Planets*, 116(E12), 2011.
[7] R.R. Ghent et al. *Geology*, 42(12):1059–1062, 2014.
[8] S.J. Robbins. *JGR: Planets*. doi: 10.1029/2018JE005592.
[9] L Rubanenko et al. 2018. doi: 2018LPICo2047.6057R.